Indocyanine green-laden poly(ethylene glycol)-*block*-polylactide (PEG-*b*-PLA) nanocapsules incorporating reverse micelles: Effects of PEG-*b*-PLA composition on the nanocapsule diameter and encapsulation efficiency

Takaichi Watanabe[1], Yui Sakamoto[1], Tetsuya Inooka[2], Yukitaka Kimura[2], and Tsutomu Ono[1]*

(1) Department of Applied Chemistry and Biotechnology, Graduate School of Natural Science and Technology, Okayama University, 3-1-1 Tsushima-naka, Kita-ku, Okayama, 700-8530, Japan Fax: +81 86 251 8083; Tel: +81 86 251 8083

(2) Division of Material and Energy Science, Graduate School of Environmental and Life Science, Okayama University, 3-1-1 Tsushima-naka, Kita-ku, Okayama, 700-8530, Japan

* Tsutomu Ono

Email: tono@okayama-u.ac.jp

Abstract

Reverse micelles are thermodynamically stable systems, with a capacity to encapsulate hydrophilic molecules in their nanosized core, which is smaller than the core generally obtained with water-in-oil-emulsion droplets. Herein, we present a simple technique for the preparation of poly(ethylene glycol)-*block*-polylactide (PEG-*b*-PLA) nanocapsules encapsulating a hydrophilic photosensitizer (indocyanine green, ICG), which exploits reverse micelle formation and subsequent emulsion-solvent diffusion. We establish the effect of the PEG-*b*-PLA composition and the co-surfactant volume on the diameter and water content of the reverse micelles. We demonstrate that the composition of PEG-*b*-PLA affects also the diameter and encapsulation efficiency of the resulting nanocapsules. We show that the ICG-laden nanocapsules fabricated under the most optimal conditions have a diameter of approximately 100 nm and an ICG encapsulation

efficiency of 58%. We believe that the method proposed here is a promising step towards the preparation of hydrophilic drug-laden polymer nanocapsules with a small diameter and therefore suitable for use in drug delivery applications based on enhanced permeability and retention (EPR) effect-driven passive targeting.

1. Introduction

Design and development of drug delivery systems for the efficient transport of drugs to a target site in the human body, with control over the drug release behavior, have received significant attention. Efficient delivery of drugs can be achieved using a multitude of suitable drug vehicles, including liposomes [1-3], polymer micelles [4-6], and polymer nanoparticles [7-10]. Among these options, biodegradable polymer nanoparticles, such as poly(ethylene glycol)-*block*-polylactide (PEG-*b*-PLA) nanoparticles with a PEG corona, have been considered as one of the most promising materials for drug delivery. The PEG corona layer prevents the adsorption of proteins and phagocytic cells on the nanoparticle surface, thereby extending significantly their potential blood circulation time [11,12]. In addition, the kinetics of the drug release from the nanoparticles can be controlled by the composition of the PLA matrix [13].

To date, PEG-*b*-PLA nanoparticles have been generally prepared by either emulsion-solvent evaporation method [14-18] or emulsion-solvent diffusion method [19-24]. Both of these nanoparticle-forming processes, however, are based on the removal of organic solvent from the precursor emulsion droplets in which the PEG-*b*-PLA nanoparticles and the drugs are dissolved. The core of the PEG-*b*-PLA nanoparticles comprises hydrophobic PLA and, therefore, these techniques are suitable for the encapsulation of hydrophobic drugs only. In contrast, the encapsulation of hydrophilic drugs in nanoparticles [25-27] has generally employed multiple emulsion systems such as water-in-oil-in-water (W/O/W) emulsions. The resulting nanoparticles are classified as "nanocapsules," with an inner aqueous core, capable of dissolving hydrophilic drugs and an external polymeric shell that serves as a barrier to diffusion. However, the PEG-*b*-PLA nanocapsules obtained using such multiple emulsion systems generally produce particles with a large diameter (over 200 nm) because of the multi-step nature of the emulsification process. Enhanced permeability and retention (EPR) effect is essential for achieving efficient drug accumulation around cancerous tumors, however, this effect is expected only for nanocarriers that are less than ca. 200

nm in size and show a prolonged circulation property [28]. Therefore, there is a growing interest in developing techniques for the preparation of PEG-*b*-PLA nanocapsules with a diameter <200 nm, and thus a high encapsulation efficiency of hydrophilic drugs.

In this paper, we propose a novel technique for obtaining PEG-*b*-PLA nanocapsules with a diameter of ca. 100 nm and a nonionic PEG surface, with a capacity to encapsulate hydrophilic photosensitizer (indocyanine green (ICG)). Fig. 1 shows the proposed method for the nanocapsule preparation, based on reverse micelle formation and oil-in-water (O/W) emulsion-solvent diffusion. To begin with, oil-soluble PEG-*b*-PLA (o-PEG-*b*-PLA) reverse micelles are prepared by dissolving o-PEG-*b*-PLA in a mixture of ethyl acetate (EA) and isopropanol (IPA) as the co-surfactant, and allowing this mixture to come into contact with pure water. In this first step, amphiphilic o-PEG-*b*-PLA molecules, dissolved in the organic phase, assemble to give reverse micelles with extremely small aqueous cores. In the second step, ICG is added to the organic solution, where the nanoscale aqueous core of the prepared reverse micelles facilitates its dissolution. In the third step, the organic phase containing the reverse micelles is emulsified with an aqueous solution containing water-soluble

PEG-*b*-PLA (w-PEG-*b*-PLA) by ultrasonication, which generates O/W emulsion nanodroplets. In the final step, the nanoemulsion is diluted with a large of pure water. Because of the high solubility of EA in water (8.7 wt% at 20 °C), the EA present in the droplet diffuses quickly into the external aqueous solution, resulting in the precipitation of ICG-laden PEG-*b*-PLA nanocapsules. The key feature of our method is the use of a reverse micelle system to drive the nanocapsule formation, as well as the incorporation of ICG as a hydrophilic molecule in these nanocapsules. Reverse micelles have the capacity to spontaneously incorporate hydrophilic molecules and their size is significantly smaller than that of typical water-in-oil (W/O) droplets. Therefore, we expect that this system will lead to improvements in the encapsulation efficiency of hydrophilic drugs and reduce the diameter of the resulting nanocapsules. In addition, PEG-*b*-PLA molecules that do not participate in forming reverse micelles in the O/W emulsion nanodroplets can adsorb to the O/W interface during preparation, and thus the resulting nanocapsules would have a nonionic PEG layer on their surfaces, which results in the enhancement of their prolonged circulation property *in vivo*. In this study, we focused specifically on investigating the effect of the preparation conditions (such as

the composition of o-PEG-*b*-PLA and the diameter of the reverse micelles) on the diameter of the resulting nanocapsules and their ability to encapsulate ICG. To the best of our knowledge, this is the first study to use polymer-based nanocapsules, fabricated using reverse micelles as the carrier for hydrophilic molecules.

2. Materials and methods

2-1. Materials

Poly(ethylene glycol) monomethyl ether (mPEG, M_n = 4,000, M_w/M_n = 1.06) was kindly supplied by NOF (Japan) and used as received. D,L-Lactide was purchased from Purac (Netherlands) and recrystallized from toluene, followed by drying under reduced pressure overnight before use. Stannous octoate ($Sn(Oct)_2$), ethyl acetate (EA), chloroform ($CHCl_3$), isopropyl alcohol (IPA), and *n*-hexane were purchased from Wako Pure Chemical Industries, Ltd. (Japan). Indocyanine green (ICG) was purchased from Tokyo Chemical Industry (Japan) and tetrahydrofuran (THF) was purchased from Kishida Chemical Co., Ltd. (Japan). Chloroform-d_1 ($CDCl_3$) was obtained from

Sigma-Aldrich (Japan). Ultrapure water was produced using a Millipore Milli-Q® purification system (EMD Millipore Corporation, USA).

2-2. Synthesis of PEG-*b*-PLA

PEG-*b*-PLA was synthesized by a ring-opening polymerization of D,L-lactide using mPEG as the initiator and $Sn(Oct)_2$ as the catalyst. Specifically, D,L-lactide, mPEG, and $Sn(Oct)_2$ (80 mg/mL) in toluene were introduced into a glass ampule, which was sealed in vacuo and heated in an oil bath at 130 °C for 24 h. Then, the ampule was broken and the reaction mixture was dissolved in chloroform (50 mL) and the precipitation of the desired polymer was achieved by the addition of *n*-hexane (400 mL) through a cotton filter. The precipitated polymer was isolated by decantation, washed with IPA, and dried in an oven under reduced pressure at 40 °C. The molecular weight distribution (M_w/M_n) of the prepared polymer samples was measured by gel permeation chromatography (GPC, HLC-8220GPC, TOSOH, Japan) at 40 °C, equipped with a refractive index detector and various columns (TSKguard column SuperH-H, TSKgel SuperHM-H, and

TSKgel SuperH2000, TOSOH, Japan). Throughout the GPC analysis, THF was used as the eluent at a flow rate of 0.6 mL/min, and the calibration curve was obtained using polystyrene standards. The chemical structure of the fabricated polymers was confirmed by ^{1}H NMR spectroscopy. The NMR analysis was carried out using a JEOL FT NMR System (JMN-AL300, JEOL, Japan) at room temperature in $CDCl_3$. The number number-average molecular weights (M_n) of the polymer samples were calculated from the corresponding ^{1}H NMR spectra.

2-3. Preparation and physicochemical characterization of o-PEG-*b*-PLA reverse micelles

EA solutions (5 mL each) containing o-PEG-*b*-PLA (3 wt%) with a varying hydrophile-lipophile balance (HLB) were prepared, followed by addition of IPA (0.1–2.0 mL). Pure water (10 mL) was slowly introduced into each sample. The samples were shaken horizontally for 24 hours at 100 rpm at room temperature, which lead to the formation of reverse micelles in the organic phase. The organic phase was gently

isolated from each sample and the water content in this organic phase was measured using a Karl Fischer Titrator (MKA-610, Kyoto Electronics, Japan). The hydrodynamic diameter of the reverse micelles was measured by dynamic light scattering (DLS) using Zetasizer Nano ZS (Malvern instruments, UK).

2-4. Preparation of ICG-laden o-PEG-*b*-PLA nanocapsules

Polymeric nanocapsules encapsulating ICG were prepared by a two-step process, where the ICG was first solubilized within the reverse micelles, followed by emulsion-solvent diffusion. First, several samples of o-PEG-*b*-PLA (3 wt%) with a different HLB value were each dissolved in EA (4 mL). A different amount of IPA, used as the co-surfactant, was added into the prepared organic solutions, followed by slow addition of pure water (10 mL) to give two-phase systems. The samples were shaken for 24 hours at 100 rpm at room temperature, which facilitated extraction of the aqueous phase into the organic phase and formation of reverse micelles in the organic phase. The organic phase (2 mL) was carefully isolated form each sample. ICG (2 mg), which is insoluble in both EA and

IPA but soluble in water, was added to the prepared organic phases. Water-soluble w-PEG-*b*-PLA (5 wt%) was dissolved in a NaOH aqueous solution (5 mL, pH = 12.0) by ultrasonication (at 20°C, 160W, 20 sec). Each organic polymer phase, now comprising the solubilized ICG, was mixed with the prepared aqueous w-PEG-*b*-PLA solution, resulting in an O/W emulsion. The prepared emulsion was diluted with a NaOH aqueous solution (40 mL, pH = 12.0), thereby inducing diffusion of EA into the continuous aqueous phase, while keeping ICG in the dispersed phase and subsequent precipitation of o-PEG-*b*-PLA nanocapsules. The nanocapsules were purified by centrifugation (82,000 g for 15 min, 3 runs), and freeze-dried overnight, affording the nanocapsules as a green powder. All steps of the preparation process were carried out in darkness in order to prevent the photo-degradation of ICG. The morphology of the prepared nanocapsules after freeze-drying was observed by means of a scanning electron microscope (SEM, S-4700, Hitachi Ltd., Japan) at a voltage intensity of 1 kV. The prepared nanocapsule samples were sputter-coated (E-1030 Ion-Sputter, Hitachi Ltd., Japan) with Pd/Pt in order to reduce the sample charging.

2-5. Physicochemical characterization of ICG-laden PEG-*b*-PLA nanocapsules

The hydrodynamic diameter and the zeta potential of the prepared nanocapsules was determined by DLS using Zetasizer Nano ZS (Malvern instruments, UK) at 25 °C. The nanocapsule samples were suspended in water and sonicated thoroughly before the measurement in order to produce a homogeneous suspension. The measured nanocapsule sizes were determined as the average value of 15 runs. The experimental values were calculated as the average of three different nanocapsule formulations. The zeta potential values of the nanocapsules were determined as the average value of 100 runs. In order to determine the encapsulation efficiency of ICG in the nanocapsules, a sample of the freeze-dried nanocapsules (2 mg) was dissolved in acetic acid (2 mL) and the solution was analyzed by UV-Vis spectroscopy (U-2000A, Hitachi, Japan) at a wavelength of 787 nm. The concentration of ICG in the sample was determined by comparison to a standard curve. All measurements were carried out under reduced lighting and the instrument operating conditions were kept constant.

3. Results and discussion

3-1. Synthesis and characterization of PEG-*b*-PLA block copolymers

We synthesized PEG-*b*-PLA diblock copolymers by a ring-opening polymerization of D,L -lactide, using mPEG as the macroinitiator. PEG is a hydrophilic and biocompatible polymer that has been used widely as a non-inflammatory modifier for proteins and drugs, whereas PLA is a hydrophobic and biodegradable polymer that has been used predominantly as a matrix in the fabrication of biomaterials. The PEG-*b*-PLA diblock copolymers synthesized in this study were characterized by ^{1}H NMR spectroscopy and GPC analysis (Fig. S1), and a summary of the results is shown in Table 1. The number-average molecular weight (M_n) and the molecular weight distribution (M_w/M_n) were determined from the ^{1}H NMR spectra and GPC analysis, respectively. In this study, we synthesized six types of PEG-*b*-PLA diblock copolymers with different length of PLA. The variation in the PLA length was achieved by changing the molar ratio of the monomer (D,L-lactide) to the initiator (PEG) during the polymerization reaction. The

obtained diblock copolymers can be classified into two groups, depending on their solubility: water-soluble PEG-*b*-PLA (w-PEG-*b*-PLA) and oil-soluble PEG-*b*-PLA (o-PEG-*b*-PLA). The water-soluble w-PEG-*b*-PLA (M_n = 4,700; M_n PEG = 4,000; M_n PLA = 700) with an HLB of 18.2 exhibits excellent surface activity between an EA and water (O/W) interface [29] and was therefore used as a polymeric surfactant to stabilize the emulsion. The five different remaining oil-soluble o-PEG-*b*-PLA copolymers (Table 1, M_n = 12,700–42,400; M_n PEG = 4,000; M_n PLA = 8,700–38,400) with an HLB in the range of 1.89–6.30 were used as the matrix in the formation of reverse micelles and nanocapsules.

3-2. Effect of the co-surfactant content on the diameter of the reverse micelles

Owing to the hydrophobic nature of the PLA segment, amphiphilic PEG-*b*-PLA copolymers can self-assemble in aqueous solutions to form micelles. Similarly, because of the hydrophilic nature of the PEG segment, PEG-*b*-PLA copolymers have the capacity to form reverse micelles in solvents. Reverse micelles are thermodynamically

stable systems with the capacity to spontaneously solubilize hydrophilic drugs within their nanosized core. In contrast, W/O emulsions are generally unstable, leading to the coalescence of all droplets over time. Thus, the use of a reverse micellar solution as the dispersed phase in the formation of hydrophilic drug-laden nanocapsules presents an efficient tool for controlling the nanocapsule diameter, compared to the use of W/O emulsions. The diameter of reverse micelles is determined by the amount of the co-surfactant and the compositions of the copolymer employed in their formation. Therefore, we first examined the effect of the co-surfactant content on the diameter of the reverse micelles. In this study, isopropyl alcohol (IPA) with a secondary alcohol group was used as the co-surfactant in order to enhance the stability of the reverse micelles [30]. The reverse micelles were prepared by shaking 5 mL of EA solution containing 3 wt% of o-PEG-*b*-PLA and IPA (0.1, 0.5, 1.0, 1.5 or 2.0 mL), and 10 mL of pure water for 24 hours. We observed that the organic phase turned slightly cloudy after 24 hours, at which point we used the organic phase to determine the diameter of the reverse micelles using DLS.

Fig. 2 shows the effect of the quantity of the co-surfactant (IPA) present in the

mixture on the diameter of the reverse micelles obtained in the EA phase. We prepared the reverse micelles using o-PEG-*b*-PLA samples with different HLB values. The experiment employing the least hydrophophilic o-PEG-*b*-PLA-1, with an HLB of 1.89, showed that the diameter of the reverse micelles in EA reaches a minimum value at 1 mL of IPA, and then increases sharply with increasing amount of IPA (up to 2 mL). More specifically, in the presence of 0.1–0.5 mL IPA, the o-PEG-*b*-PLA molecules were found to form large polymer aggregates (d > 300 nm). Increasing the IPA quantity to 1 mL resulted in the formation of the smallest reverse micelles, with a diameter of less than 100 nm. This result indicates that 1 mL of IPA is the quantity of co-surfactant that is the most suitable for the formation of stable reverse micelles with a small diameter. The steep increase in the reverse micelle size in the presence of more than 1 mL of IPA might indicate a reduced solubility of the PLA segments of o-PEG-*b*-PLA in the mixture of EA and IPA, thereby destabilizing the reverse micelles. Formation of reverse micelles using more hydrophophilic o-PEG-*b*-PLA-5, with an HLB of 6.30, revealed that the diameter of the reverse micelles remains fairly constant in the 0.1–1 mL range of IPA, and increases when the quantity of IPA is increased from 1 mL to 2 mL. These

results show that formation of small reverse micelles with o-PEG-*b*-PLA-5 requires a smaller quantity of IPA, compared to o-PEG-*b*-PLA-1. Using these experiments, we determined that the reverse micellar system that employs the IPA co-surfactant at 1 mL is the most suitable system for the preparation of small reverse micelles from o-PEG-*b*-PLA. Therefore, all experiments in the subsequent sections were carried out at using a fixed amount of IPA (1 mL) in the organic phase.

3-3. Effect of o-PEG-*b*-PLA composition on the properties of the reverse micelles

In the next step, we examined the relationship between the composition of o-PEG-*b*-PLA and the reverse micelle size and the water content. The reverse micelles were prepared by shaking 10 mL of pure water with 1 mL of IPA and 5 mL of EA solution containing 3 wt% of o-PEG-*b*-PLA with different HLB values for 24 hours. In these experiments, a higher HLB value corresponds to a lower ratio between the length of PLA and the PEG length. Fig. 3 shows the changes in the measured diameter of the reverse micelles and the water content in the reverse micellar solutions as a function of

the HLB value of o-PEG-*b*-PLA. The reverse micelle diameter was found to decrease together with an increasing value of HLB. In contrast, the water content in the reverse micellar solution exhibited an increase with increasing HLB values. Most likely, the reduction in the reverse micelle size can be attributed to the shorter length of the PLA segment in the reverse micelle core. The increase in the water content, on the other hand, probably stems from the increase in the proportion of PEG in the system. The molecular weight of o-PEG-*b*-PLA decreases with an increasing HLB value, which represents an increase in the content of the hydrophilic PEG in the system relative to the hydrophobic PLA. The reverse micelles were prepared using a given weight% of o-PEG-*b*-PLA and, therefore, an increase in the HLB value of o-PEG-*b*-PLA corresponds to an increase in the molar concentration of o-PEG-*b*-PLA in the organic phase. The PEG segments in o-PEG-*b*-PLA have a high affinity for water molecules. Expectedly, therefore, the water content in the reverse micellar solution increased with an increasing molar concentration of the PEG segments in the system. These results demonstrate that the HLB value of the employed o-PEG-*b*-PLA affects significantly the reverse micelle size and the water content in the reverse micellar solution. In summary, we established

successfully that employing the o-PEG-*b*-PLA with the highest HLB value affords reverse micelles with the smallest diameter.

3-4. Effect of o-PEG-*b*-PLA composition on the nanocapsule diameter and ICG encapsulation efficiency

ICG is a water-soluble carbocyanine dye that absorbs and fluoresces strongly in the near-infrared region of the electromagnetic spectrum, exhibiting an absorption and emission maxima at 780 and 820 nm, respectively. This molecule is frequently used as a contrast agent in biology [31-33] and as a photosensitizer in photodynamic therapy (PDT), where it produces heat and toxic chemical species such as singlet oxygen, superoxide anions, and hydroxyl radicals to destroy cancerous cells and tissues [34,35]. Incorporation of ICG in PEG-*b*-PLA nanocapsules having approximately 100 nm in diameter and a PEG surface would be able to enhance the stability of ICG *in vivo* and deliver it to the target cancerous cells and tissues through EPR effect, which would allow recipients for PDT to avoid critical side effects such as photodermatosis. We thus

prepared ICG-incorporating PEG-*b*-PLA nanocapsules using reverse micelle formation, followed by emulsion-solvent diffusion. Following the preparation of an EA solution containing the reverse micelles, 2 mg of ICG was dissolved in 2 mL of the organic phase. We found that while a control EA solution lacking the reverse micelles was not capable of dissolving ICG, the EA solution containing the reverse micelles dissolved ICG completely. The EA solution, now containing the dissolved ICG, was mixed with 5 mL of an aqueous w-PEG-*b*-PLA solution (pH 12) by sonication, resulting in an O/W emulsion. The emulsion solution was diluted with 40 mL of a basic aqueous solution (pH 12), which induced the diffusion of the EA into the aqueous phase and precipitation of the nanocapsules.

Fig. 4 shows the changes in the hydrodynamic diameter of the nanocapsules after solvent diffusion as a function of the HLB of the employed o-PEG-*b*-PLA, at a fixed volume of IPA (1 mL). The results in Fig. 4 clearly show that the hydrodynamic diameter decreases with an increasing o-PEG-*b*-PLA HLB value—an outcome, which is in good agreement with the HLB-dependent change in the size of reverse micelles, discussed previously in Fig. 3. To evaluate the surface properties of the nanocapsules,

we performed the zeta potential measurement of the nanocapsules. As shown in Table 2, we found that the zeta potential values of the obtained nanocapsules were slightly negative in the range of -2 mV to -11 mV, and that these values were in good accordance with those of nanoparticles surface modified by PEG in the previous report [36]. Combined together, these results suggest that decreasing the size of the reverse micelles is essential in order to obtain nanocapsules with a smaller diameter, and indicate that some part of PEG portions of o-PEG-*b*-PLA in the nanocapsules would be organized near the surface of the nanocapsules.

After the solvent diffusion, the nanocapsules were purified with pure water and collected by centrifugation. Fig. 5 shows the appearance of the nanocapsule dispersion after centrifugation. The green color of the resulting supernatant in the nanocapsule dispersions, prepared using o-PEG-*b*-PLA with an HLB value of 5.48 and 6.30, is indicative of ICG leakage during the centrifugation process. This leakage might be caused by the shorter length of the PLA segments in the employed o-PEG-*b*-PLA, and was significantly less noticeable in the dispersions with HLB values below 5.48. The shorter PLA length is associated with a shorter diffusion distance between the aqueous

core of the nanocapsules and the external aqueous phase [37]. Fig. 6 shows the encapsulation efficiency of ICG in the resulting nanocapsules, as determined by UV-Vis spectroscopy. We found that the highest encapsulation efficiency of 58.4% was achieved in the nanocapsules prepared using o-PEG-*b*-PLA-4 with an HLB of 4.28. From these results, we determined that o-PEG-*b*-PLA-4 is the most suitable material for both the fabrication of nanocapsules with a diameter around 100 nm and for reducing the leakage of ICG molecules during the centrifugation.

4. Conclusions

We described and successfully demonstrated a simple technique for the preparation of PEG-*b*-PLA nanocapsules incorporating a hydrophilic photosensitizer, employing (i) reverse micelle formation and (ii) solvent diffusion. This technique differs significantly from the conventional W/O/W emulsion-solvent evaporation method. By tuning the composition of o-PEG-*b*-PLA and the quantity of the co-surfactant in the reverse micelle system, we were able to generate polymer nanocapsules with a diameter of less than 100 nm. Although further research investigating the control over the release

kinetics of the incorporated drug is required, we believe that the technique proposed here is a powerful and a facile method for preparing hydrophilic drug-laden polymer nanocapsules that can be applied to drug delivery systems based on EPR effect-mediated passive targeting.

Funding

This research did not receive any specific grant from funding agencies in the public, commercial, or not-for-profit sectors.

Supplementary data

Supplementary data associated with this article can be found, in the online version.

References

[1] Y. Barenholz, C. Bombelli, M. G. Bonicelli, P. d. Profio, L. Giansanti, G. Mancini, F. Pascale, Influence of lipid composition on the thermotropic behavior and size distribution of mixed cationic liposomes, J. Colloid Interface Sci. 356 (2011) 46-53.

[2] J. Yoon, W. Jo, D. Jeong, J. Kim, H. Jeong, J. Park, Generation of nanovesicles with sliced cellular membrane fragments for exogenous material delivery, Biomaterials 59 (2015) 12-20.

[3] R. Campardelli, I. E. Santo, E. C. Albuquerque, S. V. de Melo, G. D. Porta, E. Reverchon, Efficient encapsulation of proteins in submicro liposomes using a supercritical fluid assisted continuous process, J. Supercrit Fluids 107 (2016) 163-169.

[4] R. N. Gilbreth, S. Novarra, L. Wetzel, S. Florinas, H. Cabral, K. Kataoka, J. R-. Doria, R. J. Christie, M. Baca, Lipid- and polyion complex-based micelles as agonist platforms for TNFR superfamily receptors, J. Controlled Release 234 (2016) 104-114.

[5] Z. Wang, C. Chen, Q. Zhang, M. Gao, J. Zhang, D. Kong, Y. Zhao, Tuning the architecture of polymeric conjugate to mediate intracellular delivery of pleiotropic curcumin, Euro. J. Pharm. Biopharm. 90 (2015) 53-62.

[6] K. S. Kim, W. Park, J. Hu, Y. H. Bae, K. Na, A cancer-recognizable MRI contrast

agents using pH-responsive polymeric micelle, Biomaterials 35 (2014) 337-343.

[7] N. Yoneki, T. Takami, T. Ito, R. Anzai, K. Fukuda, K. Kinoshita, S. Sonotaki, Y. Murakami, One-pot facile preparation of PEG-modified PLGA nanoparticles: Effects of PEG and PLGA on release properties of the particles, Colloids Surf. A: Physicochem. Eng. Aspects 469 (2015) 66-72.

[8] Y. Haggag, Y. A-. Wahab, O. Ojo, M. Osman, S. E-. Gizawy, M. E-. Tanani, A. Faheem, P. McCarron, Preparation and in vivo evaluation of insulin-loaded biodegradable nanoparticles prepared rom diblock copolymers of PLGA and PEG, Int. J. Pharm. 499 (2016) 236-246.

[9] K. Ogawara, T. Shiraishi, T. Araki, T. Watanabe, T. Ono, K. Higaki, Efficient anti-tumor effect of photodynamic treatment with polymeric nanoparticles composed of polyethylene glycol and polylactic acid block copolymer encapsulating hydrophobic porphyrin derivative, Euro. J. Pharm. Sci. 82 (2016) 154-160.

[10] T. Araki, K. Ogawara, H. Suzuki, R. Kawai, T. Watanabe, T. Ono, K. Higaki, Augmented EPR effect by photo-triggered tumor vascular treatment improved therapeutic efficacy of liposomal paclitaxel in mice bearing tumors with low permeable

vasculature, J. Controlled Release 200 (2015) 106-114.

[11] J. S. Tan, D. E. Butterfield, C. L. Voycheck, K. D. Caldwell, J. T. Li, Surface modification of nanoparticles by PEO/PPO block copolymers to minimize interactions with blood components and prolong circulation in rats, Biomaterials 14 (1993) 823-833.

[12] G. S. Kwon, K. Kataoka, Block copolymer micelles as long-circulating drug vehicles, Adv. Drug Deliv. Rev. 16 (1995) 295-309.

[13] K. Avgoustakis, A. Beletsi, Z. Panagi, P. Klepetsanis, A. G. Karydas, D. S. Ithakissios, PLGA-mPEG nanoparticles of cisplatin: in vitro nanoparticle degradation, in vitro drug release and in vivo drug residence in blood properties, J. Controlled Release 79 (2002) 123-135.

[14] M. Tobio, A. Sanchez, A. Vila, I. Soriano, C. Evora, J. L. V-. Jato, M. J. Alonso, The role of PEG on the stability in digestive fluids and in vivo fate of PEG-PLA nanoparticles following oral administration, Collids Surf. B: Biointerfaces 18 (2000) 315-323.

[15] X. Tang, Y. Liang, Y. Zhu, C. Xie, A. Yao, L. Chen, Q. Jiang, T. Liu, X. Wang, Y. Qian, J. Wei, W. Ni, J. Dai, Z. Jiang, W. Hou, Anti-transferrin receptor-modified

amphotericin B-loaded PLA-PEG nanoparticles cure candida meningitis and reduce drug toxicity, Int. J. Nanomed. 10 (2015) 6227-6241.

[16] S. Dou, X-. Z. Yang, M-. H. Xiong, C-. Y. Sun, Y-. D. Yao, Y-. H. Zhu, J. Wang, ScFv-decorated PEG-PLA-based nanoparticles for enhanced siRNA delivery to Her2+ breast cancer, Adv. Healthcare Mater. 3 (2014) 1792-1803.

[17] T. Takami, Y. Murakami, Development of PEG-PLA/PLGA microparticles for pulmonary drug delivery prepared by a novel emulsification technique assisted with amphiphilic block copolymers, Colloids Surf. B Biointerfaces 87 (2011) 433-438.

[18] Z. Yue, Z. You, Q. Yang, P. Lv, H. Yue, B. Wang, D. Ni, Z. Su, W. Wei, G. Ma, Molecular structure matters: PEG-b-PLA nanoparticles with hydrophilicity and deformability demonstrate their advantages for high-performance delivery of anti-cancer drugs, J. Mater. Chem. B 1 (2013) 3239-3247.

[19] M. Muranaka, K. Hirota, T. Ono, PEG-PLA nanoparticles prepared by emulsion solvent diffusion using oil-soluble and water-soluble PEG-PLA, Mater. Lett. 64 (2010) 969-971.

[20] T. Araki, Y. Kono, K. Ogawara, T. Watanabe, T. Ono, T. Kimura, K. Higaki, Formulation and Evaluation of Paclitaxel-Loaded Polymeric Nanoparticles Composed of Polyethylene Glycol and Polylactic Acid Block Copolymer, Biol. Pharm. Bull. 35 (2012) 1306-1313.

[21] E. Ayano, M. Karaki, T. Ishihara, H. Kanazawa, T. Okano, Poly(N-isopropylacrylamide)-PLA and PLA blend nanoparticles for temperature-controllable drug release and intracellular uptake, Colloids Surf. B Biointerfaces 99 (2012) 67-73.

[22] A. Imbrogno, E. Piacentini, E. Drioli, L. Giorno, Preparation of uniform poly-caprolactone microparticles by membrane emulsification/solvent diffusion process, J. Membrane Sci. 467 (2014) 262-268.

[23] C. Bouaoud, S. Xu, E. Mendes, J. G. J. L. Lebouille, H. E. A. D. Braal, G. M. H. Meesters, Development of biodegradable polymeric nanoparticles for encapsulation, delivery, and improved antifungal performance of natamycin, J. Appl. Polym. Sci. 133 (2016) 43736.

[24] Y. Lee, E. Sah, H. Sah, Chemical approach to solvent removal during

nanoencapsulation: its application to preparation of PLGA nanoparticles with non-halogenated solvent, J. Nanoparticle Res. 17 (2015) 453.

[25] J. Xi, X. Qian, K. Qian, Q. Zhang, W. He, Y. Chen, J. Han, Y. Zhang, X. Yang, L. Fan, Au nanoparticle-coated, PLGA-based hybrid capsules for combined ultrasound imaging and HIFU therapy, J. Mater. Chem. B 3 (2015) 4213-4220.

[26] R. H. Patel, A. S. Wadajkar, N. L. Patel, V. C. Kavuri, K. T. Nguyen, H. Liu, Multifunctionality of indocyanine green-loaded biodegradable nanoparticles for enhanced optical imaging and hyperthermia intervention of cancer, J. Biomed. Opt. 17 (2012) 046003.

[27] W. Gu, Q. Zhang, T. Zhang, Y. Li, J. Xiang, R. Peng, J. Liu, Hybrid polymeric nano-capsules loaded with gold nanoclusters and indocyanin green for dual-modal imaging and photothermal therapy, J. Mater. Chem. B 4 (2016) 910-919.

[28] H. Maeda, SMANCS and polymer-conjugated macromolecular drugs: advantages in cancer chemotherapy, Adv. Drug Deliv. Rev. 6 (1991) 181-202.

[29] T. Watanabe, T. Ono, Y. Kimura, Continuous fabrication of monodisperse polylactide microspheres by droplet-to-particle technology using microfluidic

emulsification and emulsion-solvent diffusion, Soft Matter 7 (2011) 9894-9897.

[30] V. Sabale, S. Vora, Formulation and evaluation of microemulsion-based hydrogel for topical delivery, Int. J. Pharm. Investig. 2 (2012) 140-149.

[31] T. Desmettre, J. M. Devoisselle, S. Mordon, Fluorescence properties and metabolic features of indocyanine green (ICG) as related to angiography, Surv. Ophthalmol. 45, (2000) 15-27.

[32] T. P. Gustafson, S. A. Dergunov, W. J. Akers, Q. Cao, S. Magalotti, S. Achilefu, E. Pinkhassik, M. Y. Berezin, Blood triggered rapid release porous nanocapsules, RSC Adv. 3 (2013) 5547-5555.

[33] B. Quan, K. Choi, Y-. H. Kim, K. W. Kang, D. S. Chung, Near infrared dye indocyanine green doped silica nanoparticles for biological imaging, Talanta 99 (2012) 387-393.

[34] Y. Tang, A. J. McGoron, Combined effects of laser-ICG photothermotherapy and doxorubicin on ovarian cancer cells, J. Photochem. Photobiol. B, Biol. 97 (2009) 138-144.

[35] L. Wu, S. Fang, S. Shi, J. Deng, B. Liu, L. Cai, Hybrid polypeptide micelles

loading indocyanine green for tumor imaging and photothermal effect study, Biomacromol. 14 (2013) 3027-3033.

[36] R. Gref, M. Lück, P. Quellec, M. Marchand, E. Dellacherie, S. Harnisch, T. Blunk, R. H. Müller, 'Stealth' corona-core nanoparticles surface modified by polyethylene glycol (PEG): influences of the corona (PEG chain length and surface density) and of the core composition on phagocytic uptake and plasma protein adsorption, Colloids Surf. B: Biointerfaces 18 (2000) 301-313.

[37] Q. Xu, M. Hashimoto, T. T. Dang, T. Hoare, D. S. Kohane, G. M. Whitesides, R. Langer, D. G. Anderson, Preparation of monodisperse biodegradable polymer microparticles using a microfluidic flow-focusing device for controlled drug delivery, Small 5 (2009) 1575-1581.

Table 1 Characterization of the synthesized PEG-*b*-PLA copolymers, each with a different HLB value.

Sample	M_n			M_w/M_n	HLB	Solubility
	Diblock	PLA	PEG			
o-PEG-*b*-PLA-1	42,400	38,400	4,000	1.08	1.89	Oil-soluble
o-PEG-*b*-PLA-2	28,700	24,700	4,000	1.32	2.79	Oil-soluble
o-PEG-*b*-PLA-3	18,700	14,700	4,000	1.49	4.28	Oil-soluble
o-PEG-*b*-PLA-4	16,800	12,800	4,000	1.47	5.48	Oil-soluble
o-PEG-*b*-PLA-5	12,700	8,700	4,000	1.28	6.30	Oil-soluble
w-PEG-*b*-PLA	4,400	400	4,000	1.07	18.2	Water-soluble

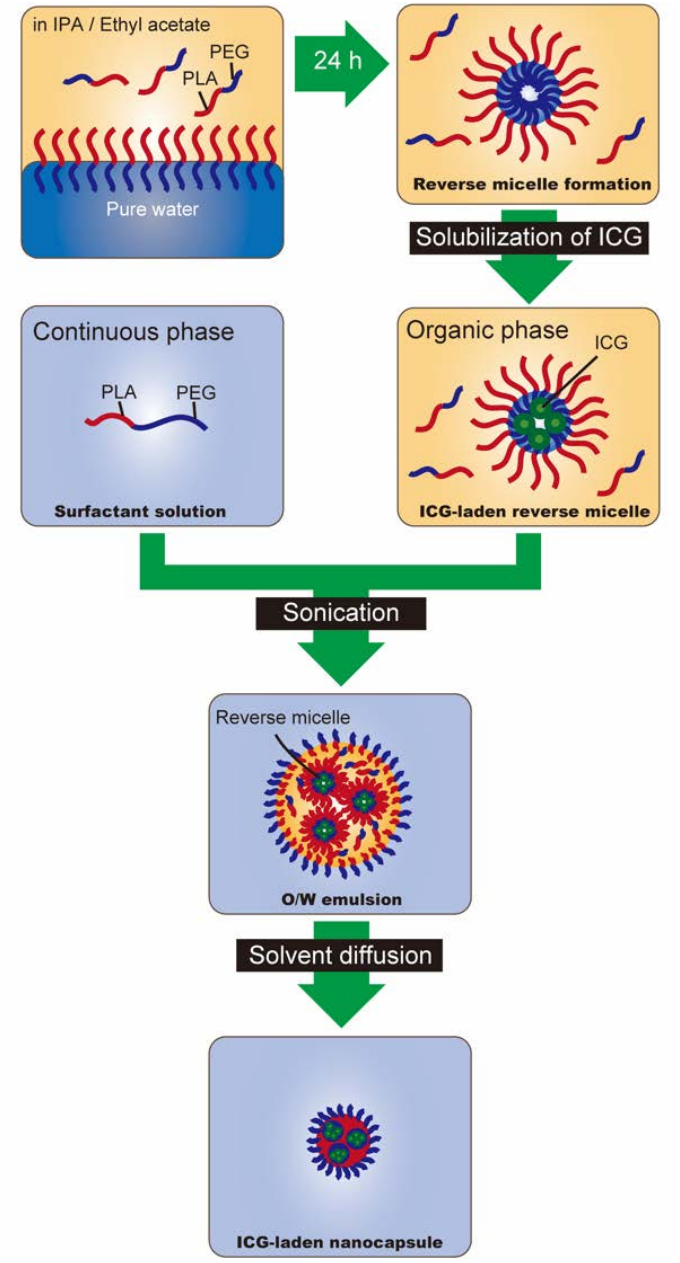

Fig. 1 A diagram illustrating the preparation of ICG-laden PEG-*b*-PLA nanocapsules by initial solubilization of ICG within reverse micelles, followed by an O/W emulsion-solvent diffusion.

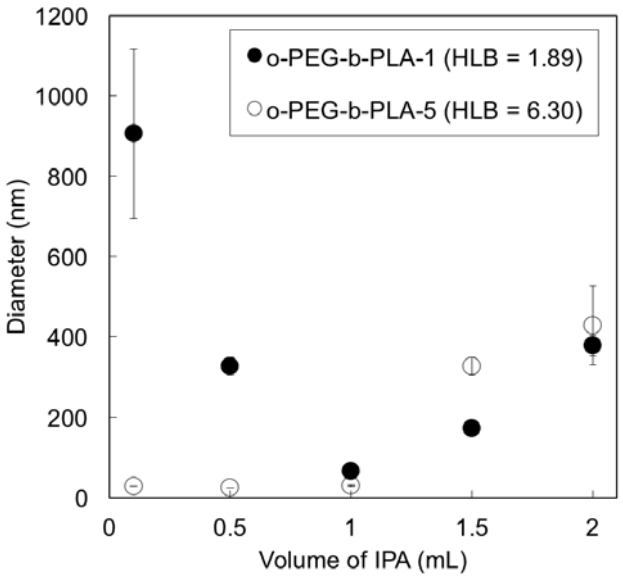

Fig. 2 Average diameter of reverse micelles fabricated using o-PEG-*b*-PLA with an HLB of 1.89 (full black circles) or 6.30 (empty white circles) in the organic phase, and an increasing amount of IPA (0–2 mL), as determined by dynamic light scattering. The volume of EA was fixed at 5 mL.

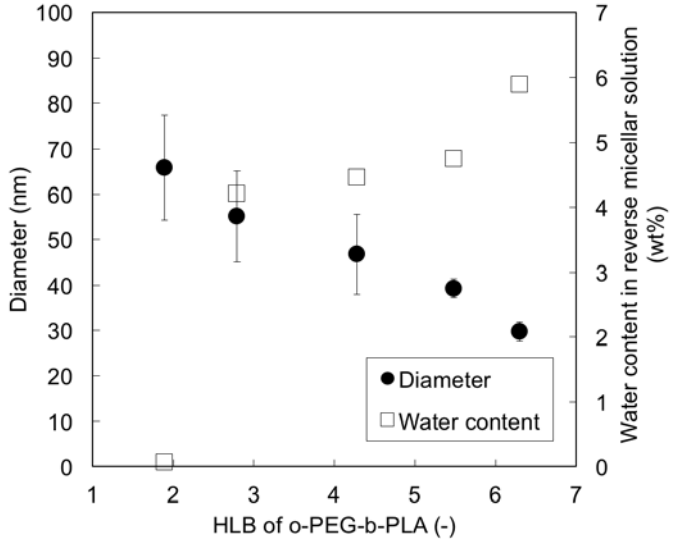

Fig. 3 Average diameter of the reverse micelles (full black circles) and the water content in the reverse micellar solutions (empty white squares) determined as a function of the HLB values of the o-PEG-*b*-PLA employed in the fabrication process.

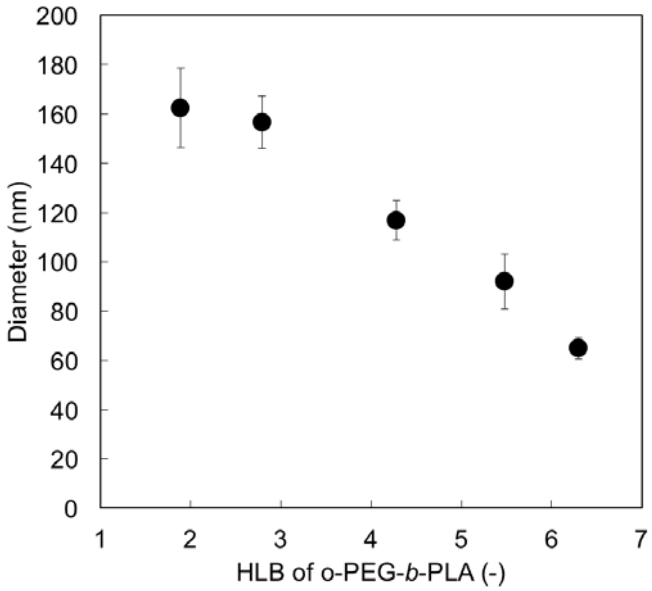

Fig. 4 Relationship between the HLB value of o-PEG-*b*-PLA and the diameter of the resulting nanocapsules.

Table 2 Zeta potential values of the resulting nanocapsules composed of PEG-*b*-PLA having a different HLB value.

Nanocapsule	HLB	Zeta potential [mV]
o-PEG-*b*-PLA-1	1.89	-10.1
o-PEG-*b*-PLA-2	2.79	-7.2
o-PEG-*b*-PLA-3	4.28	-4.3
o-PEG-*b*-PLA-4	5.48	-2.9
o-PEG-*b*-PLA-5	6.30	-5.2

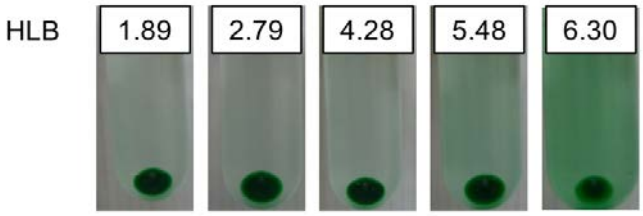

Fig. 5 Appearance of the nanocapsule dispersion after centrifugation, showing the increasing leakage of ICG into the supernatant with increasing value of HLB (left to right).

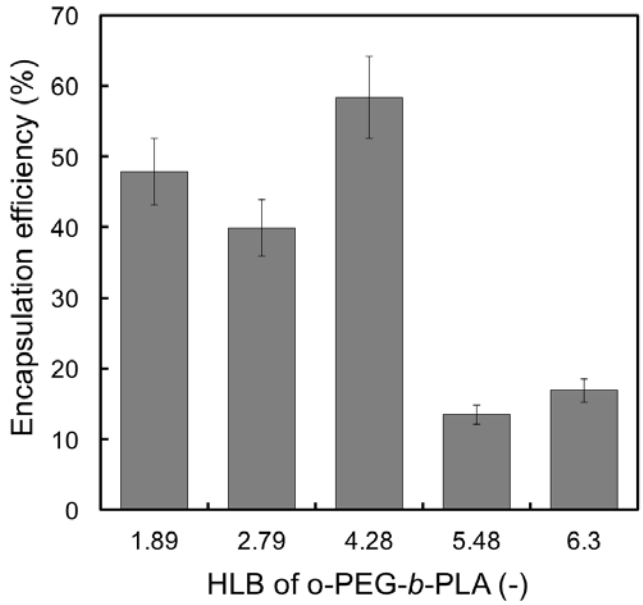

Fig. 6 Encapsulation efficiency of ICG determined for nanocapsules prepared using o-PEG-*b*-PLA with different values of HLB.